

Origins of

This content has been downloaded from IOPscience. Please scroll down to see the full text.

Download details:

IP Address: 128.138.41.170

This content was downloaded on 14/07/2015 at 11:17

Please note that terms and conditions apply.

## Origins of $k\phi$ errors for [001] GaAs/AlAs heterostructures

D. M. Wood<sup>1</sup>( $\sphericalangle$ ), A. Zunger<sup>1</sup>( $\sphericalangle$ ) and D. Gershoni<sup>2</sup>

<sup>1</sup> National Renewable Energy Laboratory - Golden, CO 80401, USA

<sup>2</sup> Department of Physics, Technion-Israel Institute of Technology - Haifa, 32000, Israel

(received 5 September 1995; accepted in final form 3 January 1996)

PACS. 73.20Dx { Electron states in low-dimensional structures (including quantum wells, superlattices, layer structures, and intercalation compounds).

PACS. 71.10+x { General theories and computational techniques (including many-body perturbation theory, density-functional theory, atomic sphere approximation methods, Fourier decomposition methods, etc.).

**Abstract.** { The  $k\phi$  method + envelope function combination used for semiconductor heterostructures is based on approximations dubious under some conditions. We directly compare 8-band  $k\phi$  with pseudopotential results for [001] GaAs/AlAs superlattices and quantum wells with all  $k\phi$  input parameters directly computed from bulk GaAs and AlAs pseudopotential bands. We find generally very good agreement for zone-center hole states within  $\approx 200$  meV of the GaAs valence band maximum, but i) systematic errors deeper in the valence band and ii) qualitative errors for even the lowest conduction bands with appreciable contributions from off- $j$  zinc-blende states. We trace these errors to inadequate  $k\phi$  description of *bulk* GaAs and AlAs band dispersion away from the zone center.

Nanostructures  $\gtrsim 100\text{\AA}$  in size were until recently [1] beyond reach of the atomistic electronic structure methods used for bulk crystals, *i.e.* *direct* solution of the Schrödinger equation

$$\left[ -\frac{\hbar^2}{2m} \nabla^2 + \sum_{i;\mathbf{R}_i} v_i(\mathbf{r} - \mathbf{R}_i) \right] \psi(\mathbf{r}) = E \psi(\mathbf{r}); \quad (1)$$

with the crystal potential  $V(\mathbf{r})$  here written as a superposition of screened atomic pseudopotentials  $v_i$  for atom species  $i$ . The spectroscopy of A/B heterostructures was instead interpreted [2] using an approach so common we term it the 'standard model' (SM): the  $k\phi$  method combined with the envelope function approximation (EFA). Although the SM has been eminently successful [3], even for ultrathin systems [4], approximations on which it is based compromise its description of heterostructures. Their impact has been partially masked by fitting of its parameters to experimental data, as described below. On general grounds one expects the SM to fail for short-period superlattices but would like to know *when* (for what thicknesses) and *how* (for which states) it fails. While detailed analyses of potential

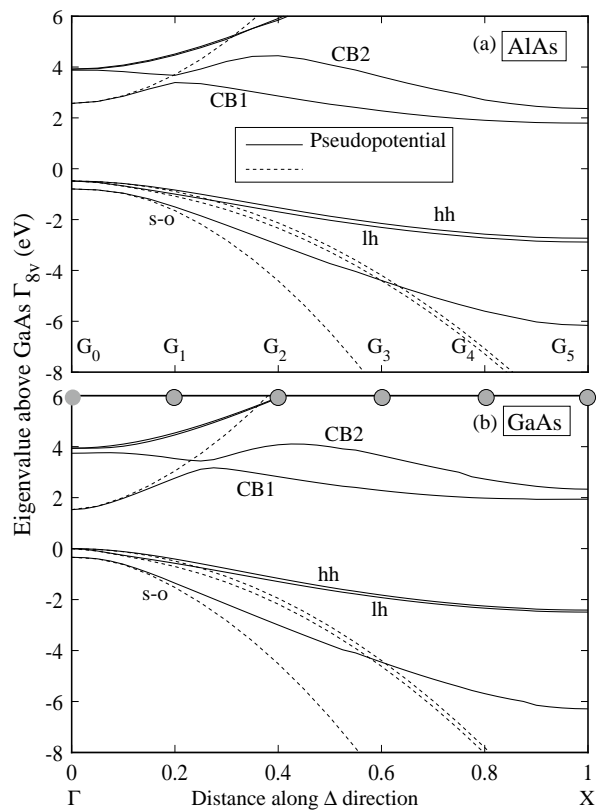
(\*) Permanent address: Department of Physics, Colorado School of Mines, Golden, CO 80401 USA; e-mail: dmwood@physics.mines.edu

(\*\*) E-mail: alex.zunger@nrel.gov

pitfalls of the SM have appeared [5], the SM cannot assess its own validity. Evaluations of actual SM errors via non-SM methods, *e.g.* tight-binding [6], generally used input data (*e.g.* effective masses) from different sources and did not necessarily reflect SM deficiencies. Only by comparing direct solutions of the fully atomistic Schrödinger equation as in eq. (1) can such errors be systematically assessed. This approach is free of approximations made in the standard model, includes full-zone dispersion of all bands, and can predict complete Bloch wave functions. We use [001] (AlAs)<sub>n</sub>(GaAs)<sub>n</sub> superlattices for  $n \cdot 20$  and (GaAs)<sub>n</sub>/AlAs quantum wells to test the standard model against a direct pseudopotential approach (eq. (1)), with the former's input parameters computed from the latter to guarantee meaningful comparison. We trace systematic errors in the SM for *heterostructures* to inadequate description of dispersion of *bulk* bands in the Brillouin zone region where coupling to off-*j* states is important.

For periodic systems the cell-periodic part  $u$  of the Bloch function  $\hat{\psi}_{n\mathbf{k}} = \exp[i\mathbf{k} \cdot \mathbf{r}]u_{n\mathbf{k}}(\mathbf{r})$  may be expanded [7] about a reference point  $\mathbf{k}_0$ :

$$u_{n\mathbf{k}}(\mathbf{r}) =$$



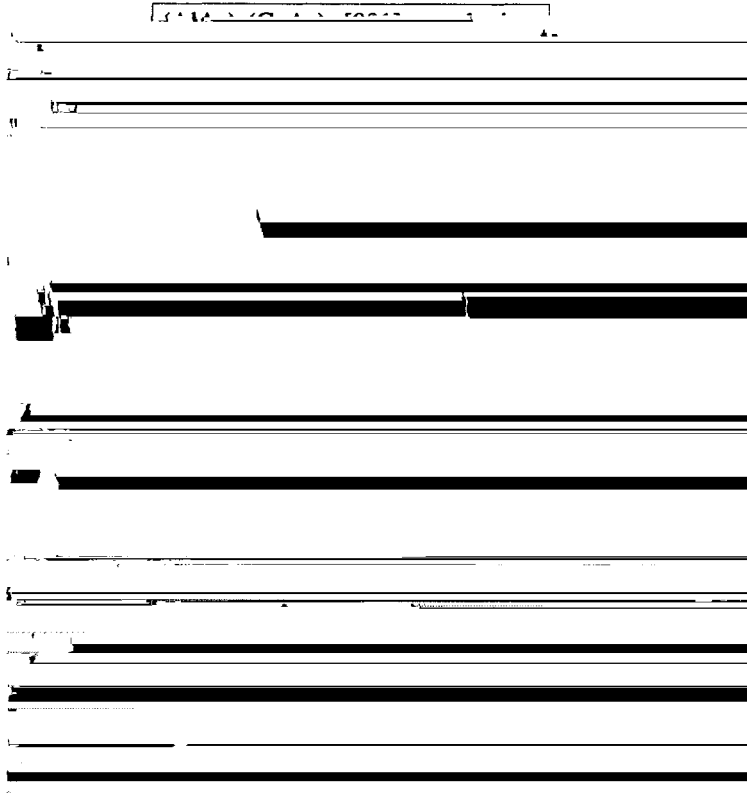


Fig. 2. { Band energies for [001] (AlAs)<sub>n</sub>(GaAs)<sub>n</sub> superlattices; *n*<sub>c</sub> indicates point of transition from indirect to direct gap system. Overbars indicate SL states which derive mainly from the ZB state in parentheses. Bulk ABP AlAs and GaAs band energies are given at right; the energy zero for *a*) and *b*) are bulk GaAs *j*<sub>6c</sub> and *j*<sub>8v</sub> states, respectively. Dashed lines show band connectivity near crossings, since *j*-*X* mixing is practically omitted.

*j*-like [14]. While the SM *X*<sub>7v</sub> GaAs valence state is almost 10 eV too low with respect to the pseudopotential value, the resulting error for heterostructure states is small because the pseudopotential *X*<sub>7v</sub>*j*<sub>8v</sub> valence band splitting is large (2.4 eV), so that interaction between heterostructure *j*- and *X*-derived valence states which fold to the heterostructure zone center is relatively weak.

Figure 2 compares zone-center ABP and SM band energies for [001] (AlAs)<sub>n</sub>(GaAs)<sub>n</sub> superlattices (SL) as a function of *n*. We label SL states via an overbar, with the ZB Brillouin zone point from which they derive in parentheses.  $\bar{j}(j)$  states derive principally from ZB *j* states, while  $\bar{j}(X_z)$  states derive mostly from folded-in zinc-blende *X*<sub>z</sub> states. Only the lowest  $\bar{j}(j)$  and  $\bar{j}(X_z)$  conduction and near-edge valence bands are shown. The extremely high energy of the SM bulk GaAs *X*<sub>6c</sub>

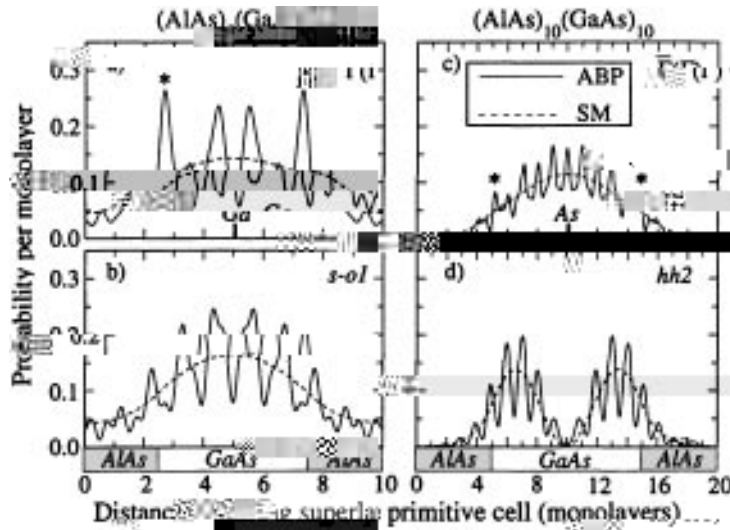


Fig. 3. { Square moduli of planar-averaged ABP Bloch states and SM envelope functions for  $\bar{j}(j)$  electron state and third hole state at  $\bar{j}$  for  $n = 5$  and  $n = 10$  SL. Odd (even)  $n$  superlattices have inversion symmetry about planes containing Ga (As) atoms. Note peaks on GaAs side of interfaces for electron states (asterisks).

ABP trends but place them *too deep* in energy; iii) for systems lacking inversion symmetry, lifting of the spin degeneracy away from the zone center is permitted in some directions. This spin splitting | absent in the SM | is significant ( $\gtrsim 30$  meV for the first heavy-hole state for  $\frac{q_{\perp}a}{2\pi} > 0.1$ ) for ‘in-plane’ dispersion in ABP calculations. SM band dispersion (not shown) agrees with ABP results only relatively near the SL zone center [13]. For  $n = 5$ , ABP values of  $m_k = m_{\gamma}$  at  $\bar{j}$  are, *e.g.*,  $\sim 3.4$  for the hh1 state and  $\sim 0.95$  for the  $\bar{j}(j_{6c})$  electron state, while SM values are 4.4 and 1.3, respectively; the anisotropy of effective masses is thus exaggerated within the SM.  $(\text{GaAs})_n/\text{AlAs}$  ( $1 \cdot n \cdot 10$ ) quantum wells show [13]  $n_c \sim 9$  (cf. fig. 2), differences in valence band dispersion, and  $1 = n^2 \bar{j}(j)$  conduction band behavior to smaller  $n$  than for superlattices (fig. 2).

Figure 3 contrasts square moduli of ABP wave functions (full lines) averaged over transverse dimensions of the primitive cell to facilitate comparisons with SM envelope functions (dashed lines), for the  $\bar{j}(j)$  electron state and the third hole state at  $\bar{j}$ . Envelope functions for states

Table I. { Projections  $P_{sG_j}$  of ABP near-edge  $(\text{GaAs})_5(\text{AlAs})_5$  states at  $\bar{j}$  ('State') onto GaAs band  $s$  labeled 'On' at the  $G_j = \frac{2\pi j}{5a}$ , and net projection  $P_s$  on band  $s$ .  $G_0$  and  $G_5$  correspond to ZB  $j$  and  $X$  points, respectively.

State	On	$G_0$	$G_1$	$G_2$	$G_3$	$G_4$	$G_5$	$P_s$
$\bar{j}(j)$	CB1	0.80	0.08	0	0.05	0.02	0	0.94
$\bar{j}(X_z)$	CB1	0	0	0.00	0.00	0.03	0.95	0.99
'hh1'	hh	0.84	0.15	0.00	0.00	0	0	1.00
'lh1'	lh	0.93	0.06	0	0	0	0	0.98
's-o1'	s-o	0.80	0.01	0	0	0	0	0.81
'hh2-a'	hh	0	0.89	0.04	0	0	0	0.93
'hh2-b'	hh	0.14	0.81	0.02	0.00	0	0	0.97
'lh2-a'	lh	0	0.93	0.02	0	0	0	0.95
'lh2-b'	lh	0.04	0.78	0.01	0	0	0	0.83

$= \sum_{s,G_j} P_{sG_j}^2$ . The net contribution  $P_s \cdot \sum_{j=0}^n P_{sG_j}$  measures how completely the SL state derives from ZB band  $s$ . Similarly, the quantity  $P \cdot \sum_{s=1}^{N_b} P_s$  measures how nearly the finite set of  $N_b$  zinc-blende bands used is 'complete' ( $P \cdot 1$ ), *i.e.* adequately describes the specified SL state.

For near-edge ABP  $(\text{AlAs})_5(\text{GaAs})_5$  superlattice states table I shows the projections  $P_{sG_j}$  onto the (spin-split) first conduction band CB1 and hh, lh, and s-o valence bands (1) | the same set used by the 8  $\mathcal{E}$

high in energy: fig. 1) are important (table I) and SM predictions *must* be too high (fig. 2) until the shortest  $G_j$  move into the CB1 quadratic region. As the period  $n$  increases, points along the zinc-blende  $\mathcal{C}$  direction which fold to  $\bar{\Gamma}$  move into the region where  $k\varphi$  adequately represents the bulk zinc-blende band structures and all near-edge superlattice states will be well described by the 'standard model'.

We have thus traced errors in the  $k\varphi$ + EFA approach to poor  $k\varphi$  description of dispersion of *bulk*